

Structure and Properties of 2,3,3,3-Tetrafluoropropene (HFO-1234yf)

Michael Feller, Karin Lux, Christian Hohenstein, and Andreas Kornath

Department of Chemistry, Ludwig-Maximilian University of Munich, Butenandtstr. 5–13, Germany

Reprint requests to Prof. Dr. Andreas Kornath. Fax: +49-89-2180-77867.

E-mail: andreas.kornath@cup.uni-muenchen.de

Z. Naturforsch. **2014**, 69b, 379–387 / DOI: 10.5560/ZNB.2014-4017

Received February 4, 2014

The novel refrigerant 2,3,3,3-tetrafluoropropene (HFO-1234yf) is discussed as a replacement for 1,1,1,2-tetrafluoroethane (R-134a) due to its low global warming potential. Although it may therefore have great potential for use on a large scale, no structural data and only a few vibrational data of the compound are known. We describe low-temperature X-ray structure analysis, vibrational spectra and combustion properties of 2,3,3,3-tetrafluoropropene. The experimental data are compared with the results of theoretical calculations. Furthermore the basic combustion properties have been investigated.

Key words: X-Ray Diffraction, Vibrational Spectroscopy, Quantum Chemical Calculation, Combustion Experiments

Introduction

HFO-1234yf (2,3,3,3-tetrafluoropropene) is currently discussed as a novel replacement for the refrigerant tetrafluoroethane in mobile air conditioners [1, 2]. Because the global warming potential (GWP) of 2,3,3,3-tetrafluoropropene ($\text{GWP}_{100} = ca. 1$) [3] is approximately 1/1300 of the GWP of R-134a (1,1,1,2-tetrafluoroethane) ($\text{GWP}_{100} = 1300$) [4], the substance is discussed as an environmentally friendly alternative. The compound was prepared for the first time by Henne *et al.* in a five-step synthesis in 1946 [5]. Later, only few studies have been reported until 2,3,3,3-tetrafluoropropene has been patented as a heat transfer reagent in 1992 and claimed as a refrigerant in 2004 [6–14]. Since then more than 600 patents have appeared. The studies of 2,3,3,3-tetrafluoropropene reported in the literature were mainly restricted to its thermodynamic properties like vapor pressure, density or heat conductivity [15–35]. Thermodynamic and heat-transporting properties are often controlled by intermolecular forces of the refrigerant molecules [36]. The investigation of these interactions can therefore improve the potentials derived from physical measurements and physicochemical modeling. Despite its importance as a potential large-scale refrigerant, the

compound was only characterized on the basis of infrared, microwave and NMR spectra [9, 11, 37–41]. This prompted us to investigate its structure and a detailed vibrational analysis as well as its basic combustion properties, which have not been reported yet.

Results and Discussion

Low-temperature single-crystal X-ray diffraction

The solid state of HFO-1234yf has not been characterized yet, since the growing of single crystals is very difficult due to the low melting point. Moreover, hydrofluorocarbons (HFCs) show often a diffraction pattern of a distorted plastic phase below their melting point [36]. Therefore several HFCs structures have been investigated by low-temperature powder X-ray diffraction. For our investigation we utilized both methods, powder and *in situ* grown single-crystal X-ray diffraction.

Single crystals of 2,3,3,3-tetrafluoropropene were grown *in situ* in a glass capillary which was mounted on a diffractometer and cooled by a nitrogen stream at a controlled temperature. The focus of the gas stream was modified by moving the capillary in the

vertical direction. Crystals were grown by decreasing the temperature slowly from -145 to -170 °C (m. p. -152.2 °C) [42]. A single crystal of the size $0.19 \times 0.13 \times 0.12$ mm³ was obtained after repeating the procedure several times. The X-ray diffraction was measured at 100(2) K. 2,3,3,3-Tetrafluoropropene crystallizes in the monoclinic space group $P2_1/n$ with 4 molecules in the unit cell (Table 1). The asymmetric unit is shown in Fig. 1.

The C=C bond length (C1–C2 1.304(7) Å) and the C–C bond length (C2–C3 1.490(6) Å) are in the range of regular carbon-carbon double and single bonds, respectively [43]. The C–F bond lengths show also no exceptions from regular C–F bonds. The carbon atoms and F1 are arranged in a plane together with F4 of the CF₃ group. The bond lengths and bond angles are compared with the results of theoretical calculations in Table 2. Overall we find a satisfactory agreement between experimental and calculated values.

The crystal packing of 2,3,3,3-tetrafluoropropene is shown in Fig. 2. The molecules display no C–H···F

contacts below the sum of the van der Waals radii (2.46 Å). In similar hydrofluorocarbons C–H···F contacts are discussed for distances between 2.46–2.64 Å. In our case we find only H···F distances of 2.773 and 2.733 Å.

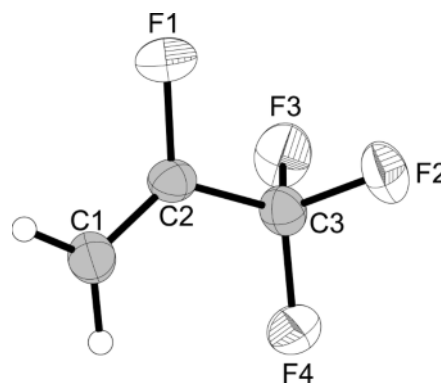


Fig. 1. Molecular structure of C₃H₂F₄ in the crystal (displacement ellipsoids at the 50% probability level).

Single-crystal diffraction data		Powder diffraction data	
Formula mass, g mol ⁻¹	C ₃ H ₂ F ₄ 114.05	Formula mass, g mol ⁻¹	C ₃ H ₂ F ₄ 114.05
Crystal system	monoclinic	Crystal system	monoclinic
Space group	$P2_1/n$	Space group	$P2_1/n$
Z	4	Z	4
a, Å	6.4246(14)	a, Å	6.4166(2)
b, Å	8.1536(14)	b, Å	8.1466(3)
c, Å	8.913(3)	c, Å	8.8799(2)
β, deg	110.80(3)	β, deg	110.82(1)
V, Å ³	436.46(17)	V, Å ³	433.86
ρ _{calcd.} , g cm ⁻³	1.74	ρ _{calcd.} , g cm ⁻³	1.73(4)
Crystal size, mm ³	0.19 × 0.13 × 0.12	Monochromator	Ge (111)
λ _{MoKα} , Å	0.71073	λ _{CuKα} , Å	1.54056
μ, mm ⁻¹	0.2	μ, mm ⁻¹	2.1
T, K	100(2)	T, K	100(2)
F(000), e	224	2θ range, deg.	10–90
hkl range	–6 : 7; –10 : 9; –10 : 10	Detector	linear PSD
Refl. measured	2073	Data points	7920
Refl. unique	831	R _p	0.04234
R _{int}	0.0308	R _{exp}	0.04458
Parameters	64	Parameters	61
R1(F) / wR2(F ²) ^a (all refl.)	0.1013 / 0.2253	R _{wp}	0.0604
Weighting scheme ^b	0.1007 / 0.9377	Program used	TOPAS Academic
S (GoF) ^c	1.103	χ ²	1.335
Residual density, e Å ⁻³	0.37 / –0.30	Background function	shifted Chebyshev
Device type	Oxford XCalibur	Diffractometer	Stoe StadiP
Solution/refinement	SHELXS-97 / SHELXL-97	Structure refinement	Rietveld method

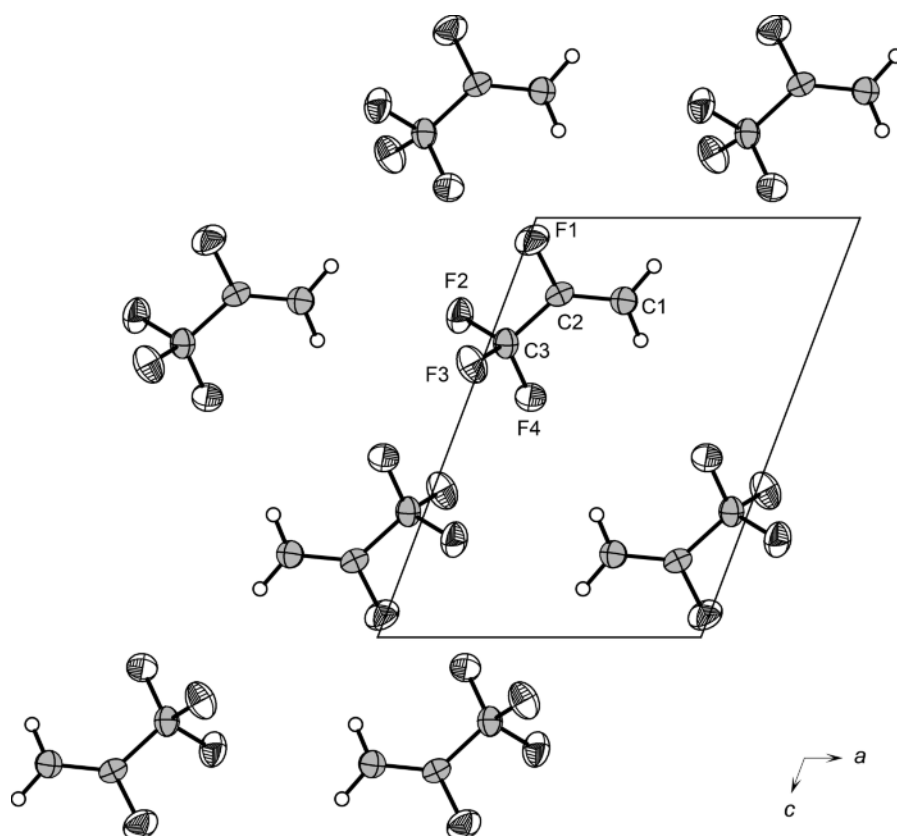
Table 1. Diffraction data and parameters of C₃H₂F₄.

^a $R1 = \sum ||F_o| - |F_c|| / \sum |F_o|$; ^b $wR2 = [\sum w(F_o^2 - F_c^2)^2 / \sum w(F_o^2)^2]^{1/2}$, $w = [\sigma^2(F_o^2) + (AP)^2 + BP]^{-1}$, where $P = (\text{Max}(F_o^2, 0) + 2F_c^2) / 3$ and A and B are constants adjusted by the program; ^c $\text{GoF} = S = [\sum w(F_o^2 - F_c^2)^2 / (n_{\text{obs}} - n_{\text{param}})]^{1/2}$, where n_{obs} is the number of data and n_{param} the number of refined parameters. Excluded region of the Rietveld refinement: 27.4–28°.

	Exp.	Calcd. ^a		Exp.	Calcd. ^a
C1–C2	1.304(7)	1.312	C3–F2	1.350(6)	1.335
C2–C3	1.490(6)	1.504	C3–F3	1.339(5)	1.335
C2–F1	1.343(5)	1.334	C3–F4	1.325(5)	1.332
C1–C2–C3	126.5(4)	126.0	F2–C3–F4	107.6(4)	108.2
C1–C2–F1	123.6(4)	123.3	F4–C3–C2	112.1(4)	111.1
F1–C2–C3	109.9(4)	110.7	F3–C3–C2	111.8(4)	110.9
F2–C3–F3	105.9(4)	107.4	F2–C3–C2	111.3(4)	110.9
F3–C3–F4	107.9(4)	108.2			
Torsion angles (deg)					
C1–C2–C3–F4	−0.5(7)	0	F1–C2–C3–F2	58.2(5)	59.6
F1–C2–C3–F4	178.7(4)	180	F1–C2–C3–F3	60.0(5)	59.6

Table 2. Selected bond lengths (Å) and bond angles (deg) of C₃H₂F₄.

^aCalculated at the M062X/aug-cc-pVTZ level of theory with the program package GAUSSIAN09 [59].

Fig. 2. Molecular packing of HFO-1234yf as seen down the crystallographic *b* axis.

Low-temperature powder X-ray diffraction

For powder X-ray diffraction the compound was transferred to a glass capillary ($d = 0.48$ mm) which was then mounted on a diffractometer and cooled by a nitrogen stream to 100 K. The diffraction pattern was recorded in Debye-Scherrer geometry. Refinement of the structural data was carried out by employing the

Rietveld method [44]. The observed, calculated and difference diffraction patterns are shown in Fig. 3.

During the low-temperature measurement ice was formed at the capillary. Therefore 5% of ice was considered in the Rietveld refinement. Below their melting points several HFCs show a diffraction pattern typical for disordered plastic phases with a body-centered cubic lattice [36]. The reflection at 27.72° appears to

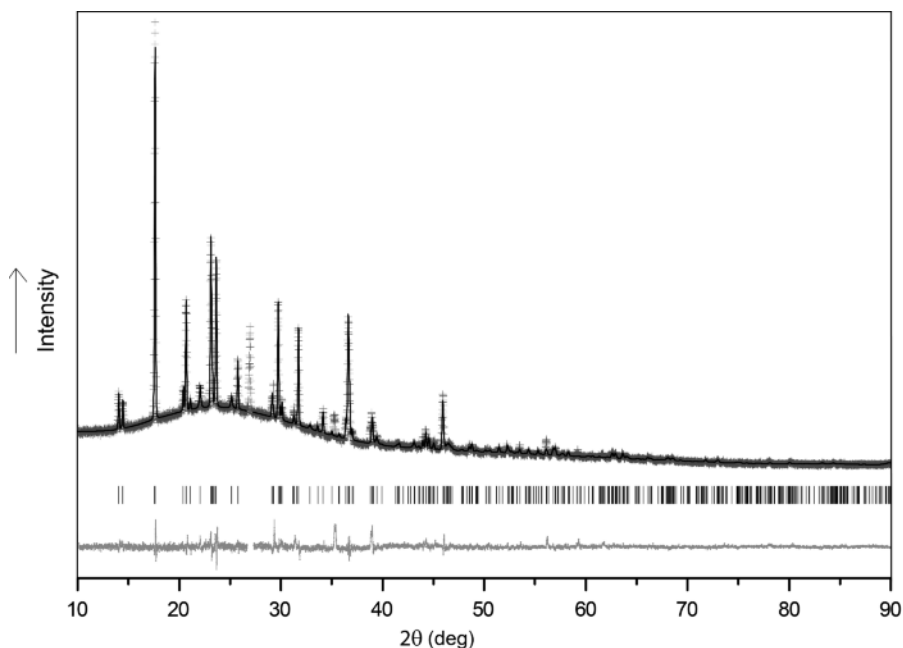


Fig. 3. Observed (crossed) and calculated (black line) powder diffraction patterns of 2,3,3,3-tetrafluoropropene, the position of Bragg reflections (vertical lines) and the difference profile (bright gray line). Excluded region $27.4\text{--}28^\circ$.

represent a disordered plastic phase and was excluded from the refinement. The cell parameters of the powder diffraction data correspond well to the single-crystal X-ray measurement, as listed in Table 1.

Raman and IR spectra of 2,3,3,3-tetrafluoropropene

The Raman spectra of all three aggregation states, and the IR spectrum of gaseous 2,3,3,3-tetrafluoropropene, are shown in Fig. 4. The vibrational data together with quantum chemically calculated frequencies are listed in Table 3. The assignments were made by comparison with previously reported IR spectra [11, 38, 39], quantum chemically calculated frequencies and consideration of the cartesian displacement coordinates. According to C_s symmetry, 21 fundamentals ($14 A' + 7 A''$) are expected for HFO-1234yf.

For the molecule 8 stretching vibrations are expected. The symmetric and antisymmetric C–H stretching vibrations are assigned at 3037 and 3160 cm^{-1} , respectively. It should be noted that in this region, typical for C–H vibrations, more Raman lines are observed than expected. Since these additional lines persist in all three aggregation states, we do not think that they arise from intermolecular interactions or crystal field splitting. The additional lines are rather

combination modes. The Raman line at 1700 cm^{-1} is assigned to the stretching vibration of the C=C double bond. The C–F stretching vibrations appear in their typical region between 1135 and 1340 cm^{-1} . The C–C stretching vibration occurs at 790 cm^{-1} as an intense Raman line. This is a rather low frequency for a C–C single bond which typically appears in the region between 850 and 1150 cm^{-1} [45]. The low C–C vibrational frequency does not indicate a weak C–C bond, since the X-ray structure analyses yield a regular C–C single bond. It is therefore caused by coupling effects which occur when a double bond is adjacent to a C–C single bond [46]. The deformation vibrations of the CH_2 group are detected at 1390 ($\delta\text{ CH}_2$), 940 ($\rho\text{ CH}_2$), 910 ($\omega\text{ CH}_2$), and 751 cm^{-1} ($\tau\text{ CH}_2$). The remaining deformation modes are observed below 670 cm^{-1} . Their assignment is listed in Table 3.

Combustion of 2,3,3,3-tetrafluoropropene

Several combustion experiments report an ignition temperature of HFO-1234yf in the region of $405\text{ }^\circ\text{C}$ [47–50]. Flammability, burning velocity and heat of combustion were determined [51], but the composition of the combustion products has not been investigated yet. Therefore we performed combustion experiments with different HFO-1234yf/oxygen mix-

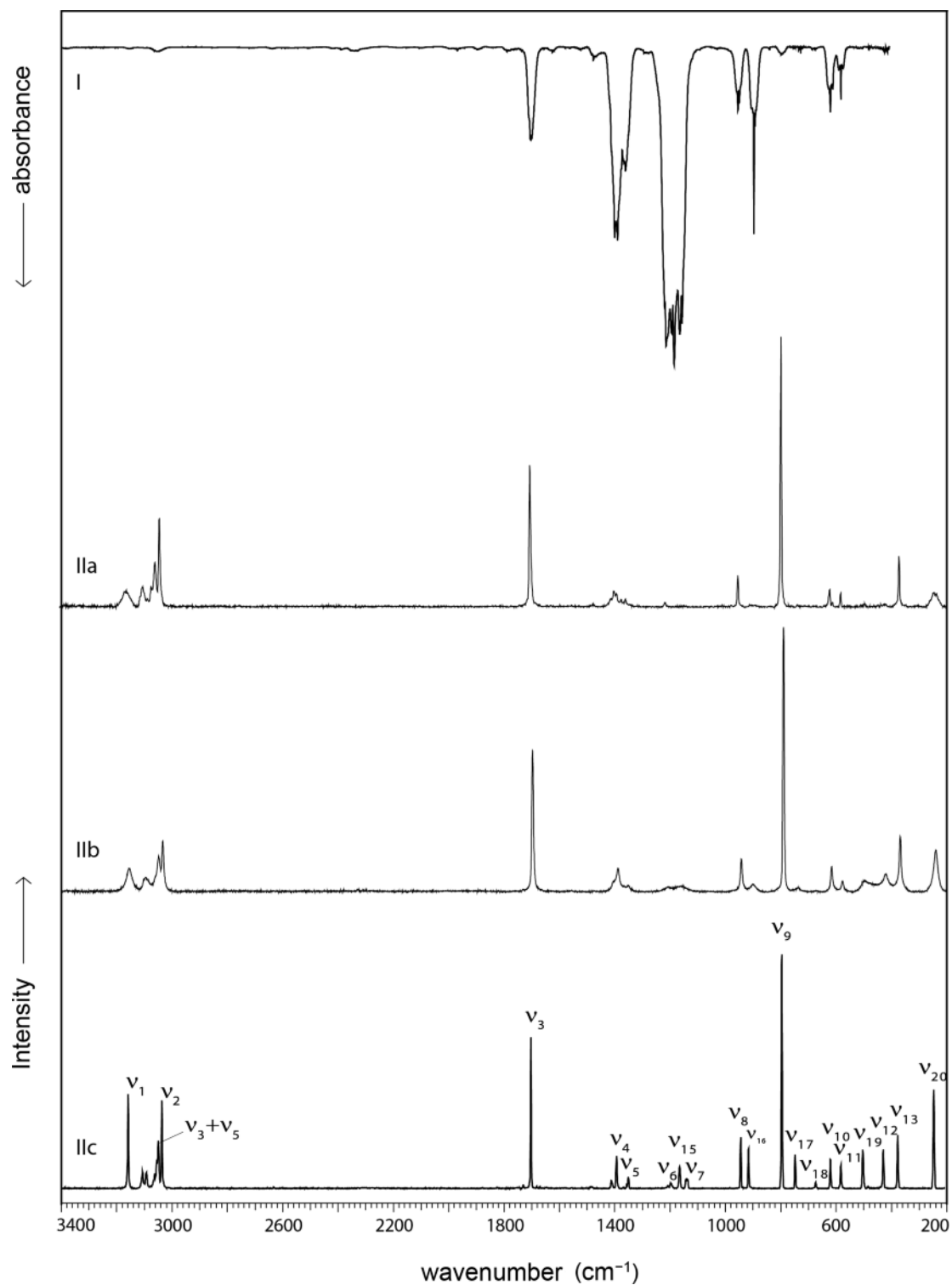


Fig. 4. Vibrational spectra of solid (IIc, 100 K), liquid (IIb, 130 K) and gaseous (IIa and I, 298 K) 2,3,3,3-tetrafluoropropene.

Table 3. Experimental and calculated frequencies of HFO-1234yf.

gaseous	Raman		IR	Calcd. ^a (Raman / IR)	Assignment	
	liquid	solid				
3161 (4)	3158 (9)	3160 (26)		3146 (38 / 3)	$\nu_{\text{as}}(\text{CH}_2)$	$\nu_1(\text{A}')$
3099 (6)	3098 (5)	3107 (5) 3094 (5) 3062 (6) 3056 (12)				
3069(6)	3050 (13)	3050 (16)				$\nu_3 + \nu_5$
3055 (13)	3036 (19)	3037 (23)	3055 (vw)	3049 (91 / 6)	$\nu_{\text{s}}(\text{CH}_2)$	$\nu_2(\text{A}')$
1701(52)	1698 (53)	1700 (67)	1700 (w)	1710 (39 / 51)	$\nu(\text{C}=\text{C})$	$\nu_3(\text{A}')$
1408 (3)		1408 (4)				
1393(5)	1388 (9)	1390 (8)	1391 (m)	1370 (7 / 130)	$\delta(\text{CH}_2)$	$\nu_4(\text{A}')$
1363 (2)	1352 (2)	1347 (10)	1357 (m)	1340 (4 / 60)	$\nu(\text{CF})$	$\nu_5(\text{A}')$
1211 (2)	1208 (2)	1192 (5)	1210 (vs)	1202 (2 / 294)	$\nu_{\text{as}}(\text{CF}_3)$	$\nu_6(\text{A}')$
			1190 (vs)			
	1162 (2)	1161 (6)	1181 (vs)	1170 (3 / 299)	$\nu_{\text{as}}(\text{CF}_3)$	$\nu_{15}(\text{A}'')$
			1160 (vs)			
		1134 (6)	1152 (s)	1135 (0.3 / 179)	$\nu_{\text{s}}(\text{CF}_3)$	$\nu_7(\text{A}')$
949 (11)	942 (3)	938 (29)	945 (w)	927 (4 / 23)	$\rho(\text{CH}_2)$	$\nu_8(\text{A}')$
	902 (3)	910 (20)	889 (w)	909 (3 / 47)	$\omega(\text{CH}_2)$	$\nu_{16}(\text{A}'')$
793 (100)	790 (100)	790 (100)	793 (vw)	778 (10 / 2)	$\nu(\text{C}-\text{C})$	$\nu_9(\text{A}'')$
	736 (2)	741 (10)		736 (0.2 / 0.5)	$\tau(\text{CH}_2)$	$\nu_{17}(\text{A}'')$
				666 (0.2 / 1)	$\delta(\text{CCC})$ o.o.p.	$\nu_{18}(\text{A}'')$
617 (7)	616 (10)	614 (21)	615 (w)	594 (2 / 21)	$\delta(\text{CCF})$ i.p.	$\nu_{10}(\text{A}')$
578 (4)	576 (4)	576 (15)	579 (vw)	556 (1 / 11)	$\delta_{\text{s}}(\text{CF}_3)$	$\nu_{11}(\text{A}')$
	497 (4)	497 (20)		482 (1 / 1)	$\delta_{\text{as}}(\text{CF}_3)$	$\nu_{19}(\text{A}'')$
	421 (7)	423 (27)		405 (1 / 1)	$\delta(\text{CCC})$ i.p.	$\nu_{12}(\text{A}')$
366 (20)	367 (21)	370 (40)		351 (2 / 0.5)	$\delta(\text{C}=\text{C}-\text{F})$ i.p.	$\nu_{13}(\text{A}')$
236 (6)	239 (16)	237 (31)		228 (1 / 0.1)	$\delta(\text{CF}_3)$	$\nu_{20}(\text{A}'')$
				225 (0.2 / 1)	$\delta(\text{H}_2\text{CFC}/\text{CF}_3)$	$\nu_{14}(\text{A}')$
				60 (1 / 1)	$\tau(\text{C}-\text{C})$	$\nu_{21}(\text{A}'')$

^a Calculated at the M062X/aug-cc-pVTZ level of theory with the program package GAUSSIAN09 [59]. Raman activity is stated on a scale of 1 to 100. Raman intensities in $\text{\AA}^4 \mu^{-1}$ and IR intensities in km mol^{-1} .

tures. The combustion products were analyzed by FT-IR spectroscopy. The recorded IR spectra of a typical experiment are shown in Fig. 5.

Carbon dioxide, carbonyl fluoride and hydrogen fluoride were found as typical combustion products. It should be noted that the quantitative analysis of HF by infrared spectroscopy is difficult since HF forms oligomers, with the equilibrium depending on the pressure, and leading to a larger variation of the band shape. Therefore, HF was detected indirectly as SiF_4 which was formed in a subsequent reaction with the glass wall of the reaction vessel. Furthermore minor amounts of CF_4 (around 5%) were observed.

At a stoichiometric ratio of oxygen and HFO-1234yf the combustion proceeds according to Eq. (1).



An excess of oxygen does not change the composition of the combustion products. At a substoichiomet-

ric ratio of oxygen the formation of COF_2 increases while a part of HFO-1234yf remains unchanged. At first sight the formation of COF_2 is unusual for hydrofluorocarbon combustion. The reason for the COF_2 formation is the F to H ratio in the molecule. The H and F atoms combine during combustion preferentially to HF which is thermodynamically favored. The remaining F atoms remain bonded to the carbon atoms and therefore COF_2 is formed as one combustion product. The COF_2 formation is not observed in case of saturated fluorohydrocarbons, because these compounds show usually no flammability when the F to H ratio is 1 or larger. At F to H ratios below 1, all fluorine atoms form HF as the combustion product.

The flammability of HFO-1234yf is unusual for a hydrofluorocarbon with an F to H ratio larger than 1. It has been discussed controversially, because it is an important safety issue for a mobile air conditioner. The reason for the flammability or with other words, instability to-

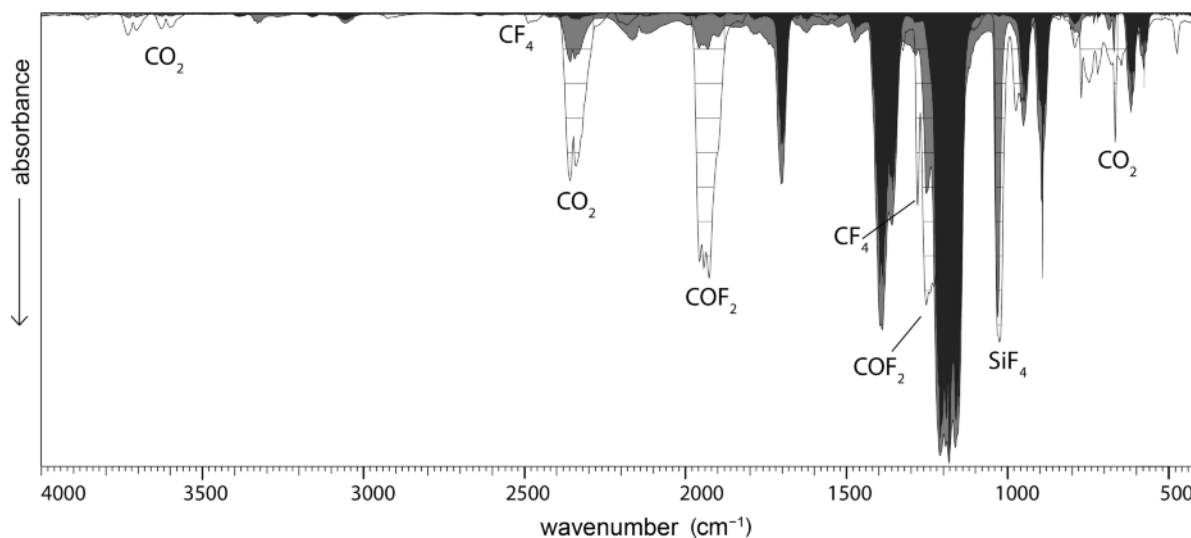


Fig. 5. FT-IR spectra of neat 2,3,3,3-tetrafluoropropene (black) and combustion products of HFO-1234yf at a stoichiometric oxygen level (white grid) and substoichiometric oxygen ratio of 1 : 2 (grey).

wards oxidative media is the presence of a C=C double bond. This instability is reflected in the short half life of the molecule in the atmosphere (*ca.* 10 days), where it is slowly attacked by OH radicals [39, 51, 52].

The combustion products of HFO-1234yf are an important safety issue for mobile air conditioner, especially for the case of fire. To our knowledge risk assessment studies for HFO-1234yf only consider the formation of HF. If COF₂ is mentioned as a potential combustion product, it is assumed that it undergoes a rapid hydrolysis with formation of CO₂ and HF. Therefore it is claimed to be irrelevant for safety issues. To our knowledge the hydrolysis kinetics of COF₂ have not been investigated yet, but from laboratory practice it is known that COF₂ does not undergo an immediate hydrolysis under contact with water. Since the toxicity of COF₂ is much larger than that of HF, and our studies have shown that COF₂ is formed as one major combustion product, it should be considered in safety risk analyses.

Conclusion

The crystal structure of 2,3,3,3-tetrafluoropropene was investigated by *in situ* single-crystal and powder X-ray diffraction. Raman spectra were recorded also for all three aggregation states. The structural parameters and vibrational modes of 2,3,3,3-tetrafluoropropene are compared with the results of

theoretical calculations. Combustion experiments of 2,3,3,3-tetrafluoropropene show carbon dioxide, hydrogen fluoride and carbonyl fluoride as combustion products. The formation of carbonyl fluoride as a combustion product is rarely observed, because a fluorohydrocarbon usually has to have an F to H ratio smaller than one to be flammable. 2,3,3,3-Tetrafluoropropene is flammable despite an F to H ratio larger than one because of the C=C double bond. The highly toxic carbonyl fluoride has to be considered in safety risk analyses.

Experimental Section

Vibrational spectra of HFO-1234yf

2,3,3,3-Tetrafluoropropene (99.8% from ABCR) was used without further purification. The purity of the compound was determined by ¹H, ¹³C and ¹⁹F NMR spectroscopy and a GC-MS analysis. The Raman spectra of liquid, solid and gaseous HFO-1234yf were recorded using the regular lateral entrance slit of a Jobin Yvon ISA T64000 spectrometer and an argon ion laser (Stabilite 2017, Spectra Physics, λ = 514.5 nm) as irradiation source.

X-Ray structure determination

The low-temperature single-crystal X-ray diffraction of HFO-1234yf was performed on an Oxford XCalibur3

diffractometer equipped with a Spellman generator (voltage 50 kV, current 40 mA) and a KappaCCD detector operating with MoK α radiation ($\lambda = 0.7107 \text{ \AA}$). Data collection at 100 K was performed using the CRYSA LIS CCD software [53]. The data reduction was carried out using the CRYSA LIS RED software [54]. The solution and refinement of the structure was performed with the programs SHELXS [55, 56] and SHELXL-97 [55, 56] implemented in the WINGX software package [57] and finally checked with the PLATON software [58]. Selected data and parameters of the X-ray structure analysis are given in Table 1.

CCDC 984019 contains the supplementary crystallographic data for this paper. These data can be obtained free of charge from The Cambridge Crystallographic Data Centre via www.ccdc.cam.ac.uk/data_request/cif.

Low-temperature powder X-ray diffraction was performed on a Stoe Stadi P powder diffractometer (Stoe & Cie, Darmstadt, Germany) in Debye-Scherrer geometry using Ge (111)-monochromated CuK α_1 radiation ($\lambda = 154.056 \text{ pm}$). A linear PSD was used to obtain the energy-dispersive X-ray spectra.

Combustion experiments

Combustion experiments were performed in a glass vessel. The glass vessel contained a tantalum filament attached to an electrical feedthrough. The reacting agents were trans-

ferred through a stainless-steel line into the vessel. The combustion was initiated by rapid electrical heating of the filament. The combustion products were transferred to an IR cell and analyzed with an FT-IR spectrometer (Bruker Vertex 80 v).

Theoretical calculations

Quantum-chemical calculations were performed with the GAUSSIAN 09 program package [59], using the restricted hybrid density functional M06-2X [60] and the aug-cc-pVTZ [61] basis set. Structure optimization was performed by employing the GDIIS algorithm with very tight convergence criteria, corresponding to maximum deviations of 10^{-6} in the density matrix elements, of 10^{-6} Hartree in the energies, of 0.000002 Hartree per Bohr in the forces and of 0.000006 Bohr in the atomic cartesian displacements [62]. Vibrational analysis was performed at the fully optimized structure. Frequencies are scaled by a factor of 0.9553.

Acknowledgement

Financial support of this work by the Ludwig-Maximilian University of Munich (LMU) and the Deutsche Forschungsgemeinschaft (DFG) is gratefully acknowledged. Thanks go also to Dominik Baumann for help with the powder diffraction data.

-
- [1] B. Osterath, *Nachr. Chem.* **2012**, *60*, 732–733.
 [2] P. Trechow, W. Pester, *VDI Nachrichten* **2012**, *2*, 13.
 [3] Ø. Hodnebrog, M. Etminan, J. S. Fuglestedt, G. Marston, G. Myhre, C. J. Nielsen, K. P. Shine, T. J. Wallington, *Rev. Geophys.* **2013**, *51*, 300–378.
 [4] P. Forster, *Changes in atmospheric constituents and in radiative forcing*, Cambridge University Press, Cambridge, **2007**, pp. 129–234.
 [5] A. L. Henne, T. P. Waalkes, *J. Am. Chem. Soc.* **1946**, *68*, 496–497.
 [6] R. N. Haszeldine, B. R. Steele, *J. Chem. Soc.* **1957**, 2193–2197.
 [7] I. L. Knunyants, M. P. Krasuskaya, E. I. Mysov, *Seriya Khimicheskaya* **1960**, *8*, 1412–1418.
 [8] D. A. Rausch, Patent application, US8071826, **1961**.
 [9] R. N. Haszeldine, D. W. Keen, A. E. Tipping, *J. Chem. Soc. C* **1970**, 414–421.
 [10] I. V. Stepanov, A. I. Burmakov, B. V. Kunshenko, L. A. Alekseeva, L. M. Yagupol'skii, *Zh. Org. Khim.* **1983**, *19*, 273–279.
 [11] R. Eric Banks, M. G. Barlow, M. Nickkho-Amiry, *J. Fluorine Chem.* **1997**, *82*, 171–174.
 [12] G. L. Heard, B. E. Holmes, *J. Phys. Chem.* **2001**, *105*, 1622–1625.
 [13] I. Sadayasu, K. Noboru, K. Shigehiro, N. Masahiro, Patent application, JP 04110388 A 19920410, **1992**.
 [14] H. T. Pham, R. R. Singh, R. H. Thomas, D. P. Wilson, Patent application, WO 2004037913 A2 20040506, **2004**.
 [15] K. Tanaka, Y. Higashi, Nippon Netsubussei Gakkai, 29th, Tokyo, Japan **2008**, D103/1.
 [16] H. Ichikawa, Nippon Netsubussei Gakkai, 29th, Tokyo, Japan **2008**, pp D104/1.
 [17] G. D. Nicola, F. Polonara, G. Santori, *J. Chem. Eng. Data* **2010**, *55*, 201–204.
 [18] K. Tanaka, Y. Higashi, R. Akasaka, *J. Chem. Eng. Data* **2009**, *55*, 901–903.
 [19] G. Raabe, E. J. Maginn, *J. Phys. Chem. Lett.* **2009**, *1*, 93–96.
 [20] R. Akasaka, K. Tanaka, Y. Higashi, *Int. J. Refrig.* **2010**, *33*, 52–60.
 [21] J. S. Brown, C. Zilio, A. Cavallini, *Int. J. Refrig.* **2010**, *33*, 235–241.
 [22] M. Yoshitake, S. Matsuo, T. Sotani, Nippon Netsu Bussei Gakkai, 30th, Yonezawa, Japan **2009**, *23*, 4, A303.
 [23] S. Yamaguchi, S. Matsuo, T. Sotani, Nippon Netsu Bussei Gakkai, 30th, Yonezawa, Japan **2009**, *30*, 350–352.

- [24] K.-J. Park, D. Jung, *Int. J. Refrig.* **2010**, *33*, 553–557.
- [25] K. Tanaka, Y. Higashi, *Int. J. Refrig.* **2010**, *33*, 474–479.
- [26] C. Di Nicola, G. Di Nicola, M. Pacetti, F. Polonara, G. Santori, *J. Chem. Eng. Data* **2010**, *55*, 3302–3306.
- [27] D. Del Col, D. Torresin, A. Cavallini, *Int. J. Refrig.* **2010**, *33*, 1307–1318.
- [28] Y. Yotsumoto, R. Sugitani, S. Matsuo, T. Sotani, Nippon Netsu Bussei Gakkai Jimukyoku, 31th, Fukuoka, Japan, **2010**, *31*, 61–63.
- [29] M. Fukushima, Nippon Netsu Bussei Gakkai Jimukyoku, 31th, Fukuoka, Japan **2010**, *31*, 58–60.
- [30] Y. Kano, Y. Kayukawa, K. Fujii, H. Sato, *Int. J. Thermophys.* **2010**, *31*, 2051–2058.
- [31] L. Fedele, S. Bobbo, F. Groppo, J. S. Brown, C. Zilio, *J. Chem. Eng. Data* **2011**, *56*, 2608–2612.
- [32] N. G. Di, M. Moglie, *Int. J. Refrig.* **2011**, *34*, 1098–1108.
- [33] M. Richter, M. O. McLinden, E. W. Lemmon, *J. Chem. Eng. Data* **2011**, *56*, 3254–3264.
- [34] R. Akasaka, *Int. J. Thermophys.* **2011**, *32*, 1125–1147.
- [35] R. A. Perkins, M. L. Huber, *J. Chem. Eng. Data* **2011**, *56*, 4868–4874.
- [36] M. Brunelli, A. N. Fitch, *Z. Kristallogr. – Cryst. Mat.* **2002**, 395–400.
- [37] V. Montanari, D. D. DesMarteau, *J. Org. Chem.* **1992**, *57*, 5018–5019.
- [38] O. J. Nielsen, M. S. Javadi, M. P. Sulbaek Andersen, M. D. Hurley, T. J. Wallington, R. Singh, *Chem. Phys. Lett.* **2007**, *439*, 18–22.
- [39] V. C. Papadimitriou, R. K. Talukdar, R. W. Portmann, A. R. Ravishankara, J. B. Burkholder, *Phys. Chem. Chem. Phys.* **2008**, *10*.
- [40] I. Skarmoutsos, P. A. Hunt, *J. Phys. Chem.* **2010**, *B114*, 17120–17127.
- [41] M. D. Marshall, H. O. Leung, B. Q. Scheetz, J. E. Thaler, J. S. Muentner, *J. Mol. Spectrosc.* **2011**, *266*, 37–42.
- [42] N. Wiberg, *Holleman, Wiberg, Lehrbuch der anorganischen Chemie*, 102. ed., de Gruyter, Berlin **2007**, p. 2006.
- [43] A. Bondi, *J. Phys. Chem.* **1964**, *68*, 441–451.
- [44] H. Rietveld, *Acta Crystallogr.* **1967**, *22*, 151–152.
- [45] T. Soltner, N. R. Goetz, A. Kornath, *Eur. J. Inorg. Chem.* **2011**, 3076–3081.
- [46] J. Weidlein, K. Dehnicke, U. Müller, *Schwingungsspektroskopie: eine Einführung*, Georg Thieme Verlag, Stuttgart **1988**.
- [47] K. Takizawa, K. Tokuhashi, S. Kondo, *J. Hazard. Mater.* **2009**, *172*, 1329–1338.
- [48] B. H. Minor, D. Herrmann, R. Gravel, *Process Saf. Prog.* **2010**, *29*, 150–154.
- [49] M. E. Koban, D. D. Herrmann, *Process Saf. Prog.* **2011**, *30*, 27–34.
- [50] S. Kondo, A. Takahashi, K. Takizawa, K. Tokuhashi, *Fire Saf. J.* **2011**, *46*, 289–293.
- [51] V. C. Papadimitriou, Y. G. Lazarou, R. K. Talukdar, J. B. Burkholder, *J. Phys. Chem.* **2010**, *A115*, 167–181.
- [52] O. J. Nielsen, M. S. Javadi, M. P. Sulbaek Andersen, M. D. Hurley, T. J. Wallington, R. Singh, *Chem. Phys. Lett.* **2007**, *439*, 18–22.
- [53] CRYVALIS CCD, (version 1.171.35.1, release 16–05–2011, CrysAlis 171.NET), Oxford Diffraction Ltd., Abingdon, Oxford (U. K.) **2011**.
- [54] CRYVALIS RED, (version 1.171.35.11, release 16–05–2011, CrysAlis 171.NET), Oxford Diffraction Ltd., Abingdon, Oxford (U. K.) **2011**.
- [55] G. M. Sheldrick, SHELXS/L-97, Programs for Crystal Structure Determination, University of Göttingen, Göttingen (Germany) **1997**.
- [56] G. M. Sheldrick, *Acta Crystallogr.* **2008**, *A64*, 112–122.
- [57] L. J. Farrugia, *J. Appl. Crystallogr.* **1999**, *32*, 837–838.
- [58] A. L. Spek, *Acta Crystallogr.* **2009**, *D65*, 148–155.
- [59] M. J. Frisch, G. W. Trucks, H. B. Schlegel, G. E. Scuseria, M. A. Robb, J. R. Cheeseman, G. Scalmani, V. Barone, B. Mennucci, G. A. Petersson, H. Nakatsuji, M. Caricato, X. Li, H. P. Hratchian, A. F. Izmaylov, J. Bloino, G. Zheng, J. L. Sonnenberg, M. Hada, M. Ehara, K. Toyota, R. Fukuda, J. Hasegawa, M. Ishida, T. Nakajima, Y. Honda, O. Kitao, H. Nakai, T. Vreven, J. A. Montgomery, J. E. Peralta, F. Ogliaro, M. Bearpark, J. J. Heyd, E. Brothers, K. N. Kudin, V. N. Staroverov, R. Kobayashi, J. Normand, K. Raghavachari, A. Rendell, J. C. Burant, S. S. Iyengar, J. Tomasi, M. Cossi, N. Rega, J. M. Millam, M. Klene, J. E. Knox, J. B. Cross, V. Bakken, C. Adamo, J. Jaramillo, R. Gomperts, R. E. Stratmann, O. Yazyev, A. J. Austin, R. Cammi, C. Pomelli, J. W. Ochterski, R. L. Martin, K. Morokuma, V. G. Zakrzewski, G. A. Voth, P. Salvador, J. J. Dannenberg, S. Dapprich, A. D. Daniels, Farkas, J. B. Foresman, J. V. Ortiz, J. Cioslowski, D. J. Fox, GAUSSIAN 09, Gaussian, Inc., Wallingford, CT (USA) **2009**.
- [60] Y. Zhao, D. G. Truhlar, *Theor. Chem. Account* **2008**, *120*, 215–241.
- [61] T. H. Dunning, *J. Chem. Phys.* **1989**, *90*, 1007–1023.
- [62] P. Császár, P. Pulay, *J. Mol. Struct.* **1984**, *114*, 31–34.